



THE USE OF ANTIRESONANCES FOR ROBUST MODEL UPDATING

W. D'AMBROGIO

*Dipartimento di Energetica, Università de L'Aquila, Località Monteluco, 67040 Roio Poggio (AQ),
Italy. E-mail: dambro@ing.univaq.it*

AND

A. FREGOLENT

*Dipartimento di Meccanica e Aeronautica, Università di Roma "La Sapienza" via Eudossiana 18,
00184 Roma, Italy. E-mail: a.fregolent@dma.ing.uniroma1.it*

(Received 1 August 1999, and in final form 10 November 1999)

In this paper, an updating technique that includes antiresonances in the definition of the output residual is considered. Antiresonances are not a global system property, but are typical of each frequency response function (FRF), thus allowing the residual vector to be enlarged with data identified from additional FRFs. However, antiresonance information is not independent of mode shape information; it is rather an alternative, which is preferable for several reasons. Antiresonances can be identified from experimental FRFs with much less error than mode shapes; furthermore, correlation between test and analysis antiresonances is a good index of the correlation between test and analysis FRFs. In the implementation of the technique, matching problems arise whenever antiresonances identified from transfer FRFs are used; unlike the situation for point FRFs, the distribution of antiresonances may be significantly altered by small changes in the structural model. Such problems may be circumvented by restricting the experimental database to point FRFs; in this case, the procedure is quite robust and excellent results are obtained, although it is necessary to plan experimental testing differently from the usual modal testing, with possible impact on related costs. For this reason, a procedure to deal with transfer FRFs by establishing a correlation between test and analysis FRFs at antiresonances using frequency domain assurance criterion (FDAC), is also evaluated. The procedure is not very robust and requires special attention to give acceptable results.

© 2000 Academic Press

1. INTRODUCTION

Dynamic model updating can nowadays be considered a mature technology. Therefore, an increasing need exists to develop robust updating procedures to be used by non-specialized analysts and without stringent demands about the quality of experimental data, demands that can be difficult to meet outside the laboratory. In this context, methods based on the minimization of the input residual (i.e., the dynamic imbalance at natural frequencies or at any given frequency) such as the FRU-IT technique [1], lose some of their appeal. Although they should in theory produce unbiased parameter estimates, in practice they require very accurate frequency response functions (FRF) measurements, the selection of significant and consistent information by the analyst, and the use of sophisticated regularization techniques. On the other hand, methods based on the minimization of the output residual

(i.e., the difference between some experimental quantities (natural frequencies, mode shapes, FRFs) and the corresponding model outputs) seem easier to use. However, the implicit non-linearity and the uncertainties related to the estimation of the experimental output quantities complicate the problem.

Among the output quantities usually considered, natural frequencies are identified quite accurately, whilst this is not the case for mode shapes (and also for measured FRFs). The idea of introducing antiresonances among the output quantities follows naturally, because they are similar to natural frequencies in many aspects. Like natural frequencies, they are located along the frequency axis and can be identified from experimental FRFs with small amounts of error. Unlike natural frequencies, antiresonances are typical of each FRF; therefore, it is possible to enlarge the experimental database by measuring more FRFs, although the risk exists that some of the data obtained are non-independent. The use of antiresonances in addition to natural frequencies and mode shapes was first suggested in reference [2], but no implementation was attempted. Moreover, it was shown [3] that antiresonance sensitivities are linear combinations of the eigenvalue and mode shape sensitivities. Therefore, antiresonance information is an alternative to, and not additional to, mode shape information, antiresonances being preferable because they can be identified with much less error than mode shapes.

Another reason for including antiresonances among the output quantities lies in their importance as correlation indicators between test and analysis FRFs. The comparison of test and analysis FRFs is commonly used to check the quality of the analytical/updated model; if two FRFs have the same resonant peaks, but different antiresonances, the comparison is not satisfactory. Therefore, antiresonances directly affect the perceived test-analysis correlation level, especially for lightly damped systems.

The use of antiresonances in dynamic model updating was considered in reference [4]. It was pointed out that matching problems arise whenever antiresonances identified from transfer FRFs are used. In fact, unlike the situation for point FRFs, the distribution of antiresonances may be significantly altered by small changes in the structural model. Such problems may be circumvented by restricting the experimental database to point FRFs. Under this condition, the technique is quite robust and provides very good results, as is demonstrated in the present paper. Furthermore, the technique is also interesting for practical applications, at least when the number of parameters to be updated is limited to some dozens, which is a reasonably high number even when large models are considered.

However, the restriction of the database to point FRFs requires experimental testing to be planned differently from usual modal testing, with possible impact on related costs. To cover this issue, a procedure for dealing with antiresonances identified from transfer FRFs is analyzed; the procedure establishes a correlation between test and analysis FRFs at antiresonances using the concept of frequency domain assurance criterion (FDAC), recently formalized in references [5, 6].

The formulation of the model updating problem using antiresonances is dealt with in section 2, whilst an application using both simulated and experimental data is presented in section 3.

2. FORMULATION OF THE MODEL UPDATING PROBLEM

2.1. MODELLING ERROR

In the present paper, the problems of updating the model geometry or the mesh size are not considered explicitly. Therefore, the updated mass and stiffness matrices are

parametrically represented in the form

$$\mathbf{M} = \sum_{i=1}^{N_{p1}} (1 + m_i)\mathbf{M}_i, \quad \mathbf{K} = \sum_{i=1}^{N_{p2}} (1 + k_i)\mathbf{K}_i, \quad (1)$$

where the sets of submatrices \mathbf{M}_i and \mathbf{K}_i are assumed to be known. They can be either selected from the FE model (at element, macro-element or sub-element level), or specially developed to account for errors related to constraint and/or joint idealization. The unknowns m_i and k_i are the incremental correction factor; they can be organized in a vector \mathbf{p} , $N_p \times 1$.

With respect to damping, it can be convenient to update the damping matrix at a later or separate step [7] or even to introduce no damping related unknown [1]. In this case, a proportional damping matrix $\mathbf{C} = \alpha^*\mathbf{M} + \beta^*\mathbf{K}$ is defined, where the coefficients α^* and β^* are estimated to give a best fit with the identified modal dampings.

2.2. UPDATING METHOD

The proposed technique belongs to the family of output residual techniques. In this case, the differences between some of the experimental quantities y_{Xi} (natural frequencies, mode shapes, FRFs, antiresonances) and the corresponding model outputs y_i are minimized. The problem is strongly non-linear and several minimization strategies can be devised. Among these, the inverse sensitivity approach is very simple and can be used when no bounds are posed on the correction parameters. In this case, the problem is written as

$$\mathbf{y}_X = \mathbf{y} + \mathbf{S}\mathbf{p} \quad \text{or} \quad \mathbf{S}\mathbf{p} = \mathbf{e}, \quad (2)$$

where $\mathbf{e} = \mathbf{y}_X - \mathbf{y}$ is the error (or residual) vector and \mathbf{S} is the sensitivity (or gradient) matrix, whose ij th term is $S_{ij} = \partial y_i / \partial p_j$. Both sides of equation (2) might be pre-multiplied by a diagonal weighting matrix $\mathbf{W} = \text{diag}(w_i)$ either to normalize the error vector (for instance to consider the percentage error) or to account for uncertainties in the experimental data. Without formal changes, equation (2) can be thought to include weighting, i.e., $S_{ij} = w_i \partial y_i / \partial p_j$ and similarly on the right-hand side, leading to a weighted least-squares solution. In order to control the parameter changes and ensure numerical stability, equation (2) can be transformed to include a regularization term. Alternatively, numerical stability can be enforced by limiting the step length at each iteration, i.e., by computing the \mathbf{p} values as

$$\mathbf{p}^{(k+1)} = \mathbf{p}^{(k)} + \alpha^{(k)}[\mathbf{S}^{(k)}]^+ \mathbf{e}^{(k)}, \quad k = 0, 1, \dots, \quad (3)$$

where $^+$ denotes the generalized inverse and $\alpha^{(k)}$ is a step length control parameter (≤ 1). As usual, the iteration is stopped as soon as $\|\mathbf{p}^{(k+1)} - \mathbf{p}^{(k)}\| < \varepsilon$, where ε is a small constant.

The step length control parameter $\alpha^{(k)}$ can be chosen according to several criteria.

- to compensate for large $\|\mathbf{e}^{(k)}\|$ at start;
- to limit the maximum component of $|\mathbf{p}^{(k+1)} - \mathbf{p}^{(k)}|$;
- to limit the norm of $(\mathbf{p}^{(k+1)} - \mathbf{p}^{(k)})$.

2.3. RESIDUALS TO BE MINIMIZED

Typically, the residual vector considers natural frequencies and mode shapes. Whilst natural frequencies can be identified quite accurately, this is not true for mode shapes.

Although lower weights can be assigned to inaccurate data, they still have a strong influence on the solution because their number greatly exceeds that of accurate data.

Here it is proposed to substitute mode shape data with antiresonance data, which in many cases can be identified much more accurately. Note that it is not possible to consider antiresonances and mode shapes together, since the two sets and their sensitivities are not independent [3].

Therefore, the experimental database consists of the natural frequencies f_{X_m} , $m = 1, \dots, N_m$, and antiresonances z_{X_r} , $r = 1, \dots, N_r$, within a selected frequency range. Specifically, N_r includes all the antiresonances identified from several measured FRFs. The residual vector \mathbf{e} , $(N_m + N_r) \times 1$, can be organized as

$$\mathbf{e} = \begin{pmatrix} f_{X_1} - f_1 \\ \vdots \\ f_{X_{N_m}} - f_{N_m} \\ z_{X_1} - z_1 \\ \vdots \\ z_{X_{N_r}} - z_{N_r} \end{pmatrix} \quad (4)$$

f_1, \dots, f_{N_m} and z_1, \dots, z_{N_r} being the corresponding analytical quantities.

Accordingly, the sensitivity matrix \mathbf{S} has dimension $(N_m + N_r) \times N_p$. To obtain an overspecified problem, $(N_m + N_r)$ must be greater than N_p . Hopefully, this is obtained by increasing N_r , i.e., by increasing the number of measured FRFs.

Since natural frequencies and antiresonances are homogeneous quantities identified with similar amounts of error, there is no need to weight equations according to data inaccuracy. Eventually, weights can be introduced to normalize the residual vector so that each term represents the percentage deviation from the test data, being divided by the corresponding experimental quantity. The weighting matrix \mathbf{W} is therefore

$$\mathbf{W} = \begin{bmatrix} f_{X_1} & & & & & & & \\ & \ddots & & & & & & \\ & & f_{X_{N_m}} & & & & & \\ & & & z_{X_1} & & & & \\ & & & & \ddots & & & \\ & & & & & & z_{X_{N_r}} & \\ & & & & & & & \end{bmatrix}^{-1} \quad (5)$$

To implement the technique, some operations that are well established when natural frequencies and mode shapes are used need to be extended to antiresonances. In practice, it is necessary to

- compute the terms of the residual vector \mathbf{e} related to antiresonances, which implies
 - identification of antiresonances from experimental FRFs;
 - computation of antiresonances from the FE model;
 - matching between test and analysis antiresonances;
- compute the sensitivities of antiresonances to the parameters \mathbf{p} .

2.3.1. Identification of antiresonances from experimental FRFs

Antiresonances correspond to zeros of frequency response functions. They can be observed as dips in the FRF magnitude, associated with a phase variation of $+180^\circ$. Accordingly, antiresonances can be identified by picking such dips from the magnitude plot of a given FRF, and by checking that the phase plot exhibits a related phase increase of 180° . Although this “dip-picking” technique (similar to the “peak-picking” technique for resonances) is quite crude, the problem of identifying antiresonances has never been tackled systematically and therefore dip-picking seems to be the most readily available technique.

In order to obtain distinct FRF dips from which the antiresonance values can be easily identified, the FRF estimator $\hat{H}_1 = S_{Fa}/S_F$, S_F being the force power spectral density and S_{Fa} the force–acceleration cross-spectral density, is recommended. It yields good signal-to-noise ratio around antiresonances. A drawback of \hat{H}_1 is the poor performance around resonances due to the low force level produced by vibration exciters in this range. This drawback can be tolerated because the identification of natural frequencies is not so sensitive to noise. In fact, several FRFs may be involved in the process, e.g., by using a global curve-fitting technique. Moreover, if impact excitation is used, the force level is also good around resonances; in this case, some care is necessary to ensure that the different impacts, which are required in the averaging process for the estimation of spectral densities, always fall on the same location. In fact, antiresonances can move even for slight changes of the impact location.

If distinct FRF dips are difficult to obtain, a curve-fitting technique based on the rational fraction polynomial representation of FRFs [8, 9] can be used. In this case, the numerator and denominator polynomial coefficients are identified, and antiresonances are given by the zeros of the numerator polynomial.

Using the dip-picking technique, errors in the estimation are mainly determined by the frequency resolution of measured FRFs; for instance, if the frequency step is 1 Hz, a rounding error of ± 0.5 Hz is possible. The kind of error can be easily kept below 1% by choosing an appropriate frequency resolution; this amount of error is much lower than that normally expected for mode shapes.

2.3.2. Computation of antiresonances from the FE model

For lightly damped systems, antiresonances are only slightly affected by damping. Therefore, they can be obtained from the zeros of the undamped system, using only mass and stiffness properties.

Specifically, given l and m , the problem is to compute the zeros of the FRF term $H_{lm}(\omega)$. The FRF matrix is the inverse of the dynamic stiffness matrix:

$$\mathbf{H}(\omega) = (\mathbf{K} - \omega^2\mathbf{M})^{-1} = \frac{\text{adj}(\mathbf{K} - \omega^2\mathbf{M})}{\det(\mathbf{K} - \omega^2\mathbf{M})}. \tag{6}$$

By definition, the zeros of $H_{lm}(\omega)$ are those ω for which the numerator of $H_{lm}(\omega)$ vanishes. The numerator of $H_{lm}(\omega)$ is the lm th term of $\text{adj}(\mathbf{K} - \omega^2\mathbf{M})$, and it is given by $(-1)^{l+m} \det(\mathbf{K}^{l,m} - \omega^2\mathbf{M}^{l,m})$, where $\mathbf{K}^{l,m}$ and $\mathbf{M}^{l,m}$ are obtained from \mathbf{K} and \mathbf{M} after deleting row l and column m . Therefore, the zeros are the values of ω that satisfy

$$\det(\mathbf{K}^{l,m} - \omega^2\mathbf{M}^{l,m}) = 0. \tag{7}$$

The zeros can also be computed from the auxiliary eigenvalue problem

$$(\mathbf{K}^{l,m} - \lambda\mathbf{M}^{l,m})\mathbf{u} = 0. \tag{8}$$

If $l = m$ (point FRF), equation (8) also describes the eigenproblem of a different physical system obtained by grounding the l th degree of freedom of the original system. The eigenvalues of the auxiliary system (the zeros of $H_{ll}(\omega)$) interlace [10] the eigenvalues of the original system (the poles), thus producing the typical appearance of point FRFs.

If $l \neq m$ (transfer FRF), equation (8) no longer represents a physical vibrating system; the problem is not self-adjoint and its eigenvalues can be negative or complex, giving rise to complex zeros that must not be considered as antiresonances. Therefore, the number of antiresonances in transfer FRFs is generally lower than in point FRFs. No interlacing property [10] holds, which implies that antiresonances of transfer FRFs can be located at any frequency.

The analytical antiresonance values, in Hz, are obtained from the eigenvalues of equation (8) as

$$z_r = \frac{\sqrt{\lambda_r}}{2\pi}. \quad (9)$$

2.3.3. Matching between test and analytical antiresonances

Before updating, it is necessary to match the analytical and experimental quantities, i.e., to check that the output residual actually represents differences between consistently related quantities (e.g., between the test and analysis natural frequency of the first flexural mode and not merely between the lowest test-analysis natural frequency pair). When natural frequencies and mode shapes are used, this can be accomplished through the modal assurance criterion (MAC) [11]. Using antiresonances, a different criterion must be developed. The idea is to establish a correlation between test and analysis FRFs at antiresonances.

A correlation coefficient between measured FRFs and the corresponding column of the analytical FRF matrix can be defined similarly to the MAC. This was done almost independently by several researchers and different names were assigned to very similar quantities.

- Frequency response assurance criterion (FRAC) by Nefske and Sung [5], Ewins [12], Fregolent and D'Ambrogio [13].
- Frequency domain assurance criterion (FDAC) by Pascual *et al.* [6], who call FRAC the analogue of coordinate modal assurance criterion (COMAC).

Here the term FDAC will be used, according to the standard notation for modal testing. The FDAC can be defined for each pair of frequencies as

$$\text{FDAC}(\omega_r, \omega_s) = \frac{|\mathbf{h}^H(\omega_r)\mathbf{h}_X(\omega_s)|^2}{\|\mathbf{h}(\omega_r)\|^2\|\mathbf{h}_X(\omega_s)\|^2}, \quad (10)$$

where \mathbf{h} and \mathbf{h}_X are column vectors containing analytical and measured FRFs, and the superscript H denotes the conjugate transpose. The FDAC value is bounded between zero and one, where a value of one indicates perfect correlation between the measured dynamic deflection shape and the dynamic deflection shape of the model. To account for phase information, a different definition can be used [6, 12] which leads to FDAC values between -1 and $+1$.

For antiresonance correlation, the FDAC can be evaluated by varying ω_r among the analytical antiresonances z_r of a given FRF H_{lm} , and ω_s among the identified antiresonances z_{X_s} of the test FRF H_{Xlm} . Only antiresonance pairs whose FDAC is greater than a previously established value are considered.

Antiresonance matching is particularly important for transfer FRFs. In this case, the interlacing property does not apply; the number of antiresonances within a given frequency band and their location are *a priori* unknown. Therefore, experimental antiresonances might be located differently from analytical ones. Furthermore, analytical antiresonances can change significantly each time the structural parameters are changed. This requires a new matching at each iteration step.

On the other hand, antiresonance matching is not so critical for point FRFs: each antiresonance lies between two natural frequencies due to the interlacing property. Once natural frequencies are properly correlated, the correct matching between antiresonances is easily found.

In order to circumvent matching problems, it could be desirable to restrict the experimental database of point FRFs, i.e., to measure only FRFs on the main diagonal of the FRF matrix rather than a row or column of the same matrix, as is usual in single reference modal testing—where either the exciter or the response transducer is located in a single position while measuring different FRFs. To measure point FRFs both the exciter and the response transducer must be located in the same position; they must be moved before taking different measurements, with a possible impact on testing time and cost. The aforementioned disadvantage of restricting the experimental database to point FRFs is compensated by the following advantages:

- all antiresonances are independent: as shown by equation (8), they correspond to the natural frequencies of several distinct physical systems, each one obtained by grounding a different d.o.f. of the original system;
- for a fixed number of FRFs, the number of involved antiresonances is maximum and does not change from one iteration step to another;
- no doubt exists as to whether a dip in the FRF magnitude is an antiresonance or a minimum, whether or not the detection of the associated phase jump is hidden by noise, since the correct answer is always provided by the interlacing property.

2.3.4. Computation of antiresonance sensitivities

In view of equation (9), the derivative $\partial z_{U_r}/\partial p_s$ is

$$\frac{\partial z_{U_r}}{\partial p_s} = \frac{1}{4\pi\sqrt{\lambda_r}} \frac{\partial \lambda_r}{\partial p_s} = \frac{1}{8\pi^2 z_{U_r}} \frac{\partial \lambda_r}{\partial p_s}, \tag{11}$$

where $\partial \lambda_r/\partial p_s$, i.e., the derivative of an eigenvalue of the generally non-self-adjoint system given by equation (8), is computed following Plaut and Huseyin [14]:

$$\frac{\partial \lambda_r}{\partial p_s} = \frac{\mathbf{v}_r^H \left(\frac{\partial \mathbf{K}^{l,m}}{\partial p_s} - \lambda_r \frac{\partial \mathbf{M}^{l,m}}{\partial p_s} \right) \mathbf{u}_r}{\mathbf{v}_r^H \mathbf{M}^{l,m} \mathbf{u}_r}, \tag{12}$$

in which \mathbf{v}_r and \mathbf{u}_r denote the left and right eigenvectors of problem (8) and the superscript H denotes the conjugate transpose. It is obvious that $\mathbf{v}_r = \mathbf{u}_r$ if equation (8) represents a self-adjoint system (point FRFs).

3. APPLICATION

Figure 1 shows a sketch of a frame structure previously built and tested in the laboratory [1]. The frame is assembled from 10 steel bars with hollow rectangular cross-section (right), connected by welded joints. The long side of the section is orthogonal to the plane of the structure. The bottom and top longerons (nodes 1–6 and 8–11) are made up of single continuous bars, welded to the remaining structural members. Due to welding, there are significant uncertainties about structural properties. It can be expected that an FE model assuming ideal junctions does not correctly describe the dynamic behaviour of the test structure.

Vibration in the frequency range 0–800 Hz, out of the plane of the frame (z direction) is considered. Consequently, the structure is modelled as a three-dimensional (3-D) frame, using 3-D (12 d.o.f.s) beam elements. The Young modulus E , the Poisson ratio ν and the mass density ρ are taken as $E = 2.1 \times 10^{11} \text{ N/m}^2$, $\nu = 0.3$ and $\rho = 7800 \text{ kg/m}^3$, while cross-sectional area A , area moments I_ζ , I_η and torsional moment I_t are computed as $A = 2.24 \times 10^{-4} \text{ m}^2$, $I_\eta = 3.668 \times 10^{-8} \text{ m}^4$, $I_\zeta = 1.438 \times 10^{-8} \text{ m}^4$ and $I_t = 3.342 \times 10^{-8} \text{ m}^4$.

To select an appropriate FE mesh, a convergence test is performed on the eigenfrequencies of the model. These are computed by subdividing the frame into 16, 32 and 160 elements, yielding [1] three sets of nearly identical eigenfrequencies below 800 Hz; therefore, the coarser mesh, consisting of 16 elements and shown in Figure 1, is used.

In all the subsequent cases, the mass matrix is assumed to be correct. Therefore, only the stiffness matrix is updated. The stiffness correction factors refer to subelement matrices related to the out-of-plane dynamics, which includes torsional and out of plane flexural rigidity. Unless otherwise stated, all the elements will be updated; therefore $N_p = N_{p2} = 16$.

First, it will be demonstrated that significant alterations in the distribution of antiresonances can be produced by small changes in the model of the structure.

3.1. ANTIRESONANCE CHANGES IN TRANSFER FRFs

With reference to the frame structure of Figure 1, an original and perturbed set of stiffness correction factors (the norm of their difference is about 3%) is shown in Figure 2.

Figure 3 shows the transfer FRF H_{65} in the two cases: two new antiresonances (between the second and the third natural frequency, and between the third and the fourth one) can be noticed on the perturbed FRF (right). (Note that the 3rd dip of the original FRF (left) is just a minimum, as it is concluded from the phase plot.)

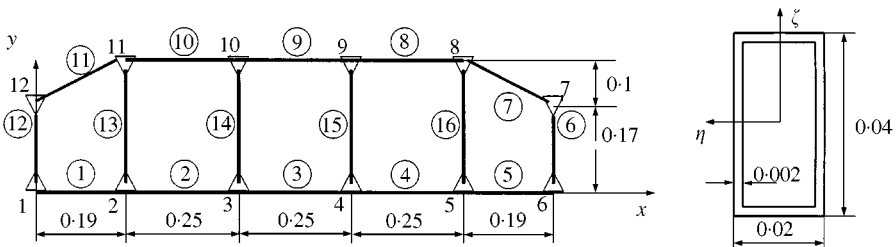


Figure 1. Test structure: nodes, elements (circled), welded joints (triangles). Bar cross-section (right).

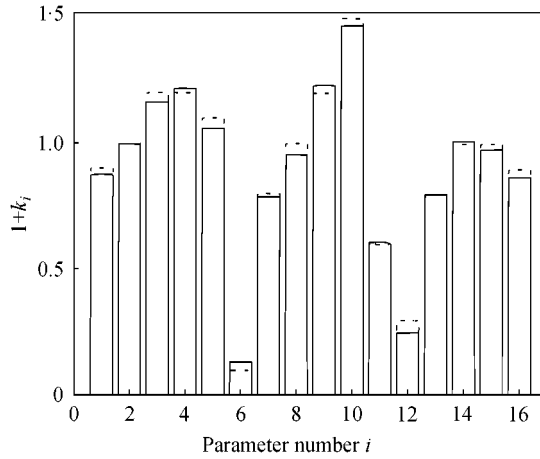


Figure 2. Stiffness correction factors: the perturbed set (dashed) is obtained by rounding the original values (solid) to one decimal digit.

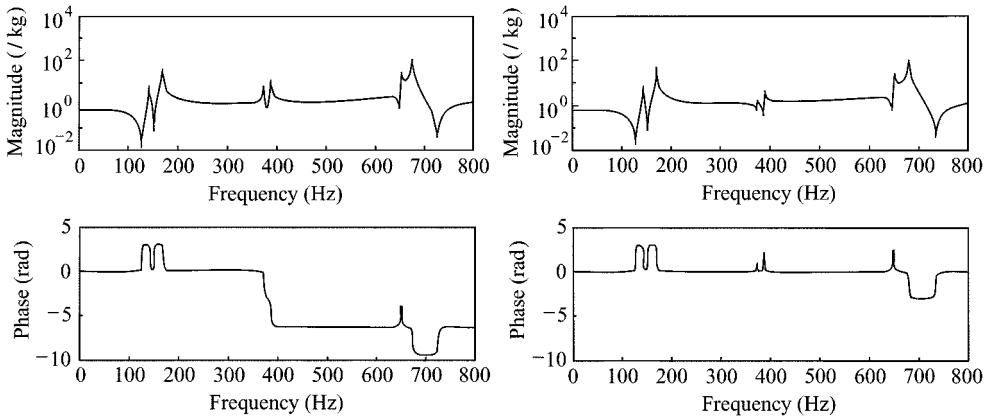


Figure 3. Transfer FRF H_{65} : (left) using the original stiffness correction factors; (right) using the perturbed correction factors.

3.2. SIMULATED TESTS

The purpose of simulated test is twofold. Firstly, it is to check that the updating procedure provides correct answers in ideal conditions. Secondly, it is to analyze the influence of some expected errors and limitations of experimental data, such as dealing with a limited number of FRFs and with identification errors on natural frequencies and antiresonances. The same kind of disturbances can be introduced in a controlled manner during simulations.

Simulated data are produced from the unperturbed stiffness correction factor k_i^X shown in the solid line in Figure 2. Two types of tests are conducted: one considering point FRFs only, i.e., the main diagonal of the FRF matrix; the second one using a traditional set of measurements, i.e., a column of the FRF matrix. In the above frequency range and direction, six natural frequencies of the system and six antiresonances for each point FRF are found.

3.2.1. Point FRFs

Table 1 shows the characteristics of the different data sets used for simulations with point FRFs. Two kinds of controlled disturbances are considered. One consists of using a limited number of FRFs for antiresonance identification; this is related to the typical limited availability of experimental data. For this reason, data sets 2, 4 and 6 consider only six over 12 point FRFs, namely those involving nodes 1–6. The second kind of disturbance consists of assuming that FRFs are only known at discrete frequency points separated by a frequency step Δf , as in actual tests. It is also assumed that natural frequencies and antiresonances are identified by peak-picking and dip-picking; i.e., their values are estimated by rounding to the nearest multiple of Δf . In data sets 3 and 4 $\Delta f = 1$ Hz, whilst in data sets 5 and 6 $\Delta f = 2.5$ Hz. Note that natural frequencies and antiresonances are exact to the fourth decimal digit in data sets 1 and 2.

Results provided by the updating technique are summarized in Table 2. To improve numerical stability, the step length control parameter $\alpha^{(k)}$, equation (3), is set to 0.1, 0.2, 0.5 in the first three iterations to compensate for large $\|e^{(k)}\|$, and it is set to 1 in the subsequent steps. The results are shown as percentage errors on the stiffness correction factors. This is only possible with simulated data, since in this case the true values of the correction factors k_i^X are known.

Data set 1 represents an ideal situation and results are expected to be almost perfect. The same holds for data set 2, because the number of data points (6 natural frequencies + 36 antiresonances) is large enough to estimate 16 unknowns.

Results obtained using data sets 3 and 4 are extremely satisfactory too. Due to the round-off errors on natural frequencies and antiresonances, the availability of a larger data set slightly improves the results. The error on the estimated parameters is of the same order of magnitude as the inaccuracy on the input data; no significant error amplification is observed.

Satisfactory results are obtained even in the worst case (data set 6), when using only six-point FRFs and a frequency step of 2.5 Hz. The error on the stiffness correction factors is less than 7%. However, a coarse frequency resolution should generally be avoided.

3.2.2. Transfer FRFs

When simulated tests are conducted using a column of the FRF matrix, the procedure used above for point FRFs, i.e., without antiresonance matching at each iteration, never

TABLE 1
Data sets for simulations with point FRFs

Data set number	1	2	3	4	5	6
No. of point FRFs	12	6	12	6	12	6
Δf (Hz)	—	—	1	1	2.5	2.5

TABLE 2

Relative error $E_k = \|\mathbf{k} - \mathbf{k}^X\|/\|\mathbf{1} + \mathbf{k}^X\|$ on stiffness correction factors using different data sets

Data set number	1	2	3	4	5	6
E_k (%)	$2.55e - 4$	$2.90e - 4$	1.9	2.57	3.9	6.71

achieves convergence. This occurs in spite of using exact values of natural frequencies and antiresonances, and of constraining the stiffness correction factors \mathbf{k} to change very slowly by selecting $\alpha^{(k)}$ in order to limit severely the maximum component of $\Delta\mathbf{k}$. Moreover, convergence is not achieved even if the initial estimate of the parameters k_i , instead of being zero, is very close to their exact values. Lack of convergence is obviously due to the use of uncorrelated quantities in the output residual. The interlacing property does not hold for transfer FRFs and the antiresonance distribution can change significantly when the parameters change during the iteration procedure.

It then becomes necessary to correlate the experimental and the analytical antiresonances using FDAC before each iteration step. Nevertheless, in this case, the correlation is not sufficient to ensure convergence unless the initial estimate of the parameters k_i is very close to their true values. Since this condition cannot be guaranteed in practical situations, a possibility is to reduce the number of structural parameters to be updated. Several parameter selection techniques exist, based on the properties of the sensitivity matrix, but none of them provides useful answers in the case considered. A further possibility is to discard the parameters that tend to diverge (i.e., those attaining physically meaningless values during the iteration procedure) to restart the procedure and to repeat the process until convergence is achieved. In this manner, only the stiffness parameters related to the elements 2, 3, 4, 6, 8, 9, 10 and 12 are selected, and the procedure converges with an error of 9.7% on structural parameters, mainly due to the uncorrected parameters 1, 5, 7, 11, 13, 14, 15 and 16, and an average error of 0.5% on natural frequencies and antiresonances. If on the contrary, parameters are arbitrarily selected, i.e., by ascribing the uncertainties due to the welded joints only to the vertical elements 6, 12, 13, 14, 15 and 16, the solution does not diverge, but shows an oscillating behaviour. Probably in this case the correlated antiresonances are different at subsequent iteration steps giving rise to cyclically different sets of equations. To avoid such situations, it should be required that the correlated set of antiresonances at a given iteration is maintained or possibly enlarged when going to the next iteration, i.e., without losing previously correlated antiresonances.

3.3. EXPERIMENTAL TESTS

Experimental data are obtained by measuring the 12-point FRFs in the z direction using impact excitation. As recommended previously, FRFs are estimated using $\hat{H}_1 = S_{Fa}/S_F$. The sampling frequency and number of samples are adjusted to get a frequency step $\Delta f = 1$ Hz. A column of the FRF matrix, corresponding to drive point 6, is also measured under the same conditions.

Natural frequencies can be identified from the experimental FRFs. In the frequency range considered, six natural frequencies are found (one repeated value at 388 Hz). By comparing them with analytical natural frequencies (Table 3) it can be concluded that dynamic model updating is necessary.

TABLE 3

Comparison between analytical and experimental natural frequencies before updating

	Natural frequencies					
Analytical (Hz)	134.0	170.2	367.1	412.0	690.4	736.9
Experimental (Hz)	145.0	170.0	388.0	388.0	661.0	703.0
Error	7.60%	- 0.13%	5.38%	- 6.19%	- 4.45%	- 4.78%

3.3.1. Point FRFs

In this case, the model is updated using antiresonances identified from point FRFs. Six antiresonances are found for each point FRF (one of them at 388 Hz). The overall number of data is $6 + 6 \times 12 = 78$. Therefore, it is possible to establish 78 equations in the 16 unknown stiffness correction factors.

The results are summarized in Figure 4 in terms of final errors on natural frequencies and antiresonances. Considering absolute values, the maximum error on natural frequencies is about 0.6% and the average error is around 0.2%, whilst for antiresonances the maximum error is about 2% and the average error is around 0.5%. These results are quite satisfactory, also considering that the average error was around 5% before updating, both for natural frequencies and antiresonances.

The quality of the updated model can be appreciated also by comparing original, test and updated FRFs (Figure 5). For the computation of updated FRFs, a proportional viscous damping matrix $\mathbf{C} = \alpha^* \mathbf{M} + \beta^* \mathbf{K}$ is used, with $\alpha^* = 6.3$ and $\beta^* = 2.2 \times 10^{-7}$ estimated to give a best fit of the identified modal dampings. The comparison concerns six FRFs. Just one of them is a point FRF (H_{66} , Figure 5(f)), whose antiresonances are explicitly considered by the updating procedure. Transfer FRFs are compared as an independent check of the quality of the results, since their antiresonances are not explicitly updated. It can be noted that the correspondence is always very good, except for H_{65} ; in this case the updated model produces two new antiresonances in the frequency range 300–400 Hz. However, this does not necessarily imply large errors in the updated parameters; it was in fact observed (Figures 2 and 3) that the antiresonance distribution of H_{65} was significantly changed by perturbing the parameters of about 3%. Therefore, it seems that the distribution of antiresonances of H_{65} is particularly sensitive to small parameter changes. The observed discrepancy can be ascribed to this fact rather than to substantial errors in the updated parameters or to the choice of non-physical parameters.

Finally, the updated stiffness correction factors are shown in Figure 6, compared with the stiffness correction factors obtained for the same structure [1] using a different updating technique (the FRU-IT technique), and a different set of measurements (a column of the FRF matrix corresponding to drive point 6, obtained using random excitation and the \hat{H}_2 estimator). In both cases, the updated stiffness of the vertical elements 6 and 12 is much smaller than the one originally estimated considering ideal junctions; this large variation is probably due to welding faults. Also, the stiffness of the other vertical elements (13–16) is

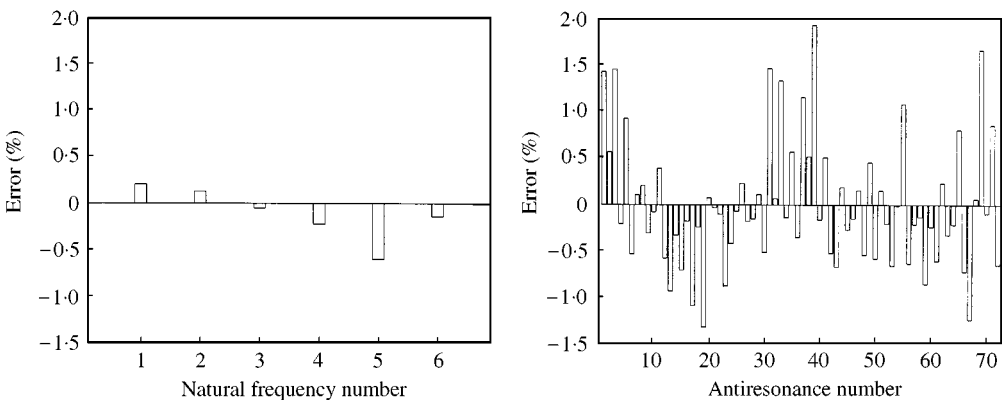


Figure 4. Final errors on natural frequencies (left) and antiresonances (right) using antiresonances identified from point FRFs.

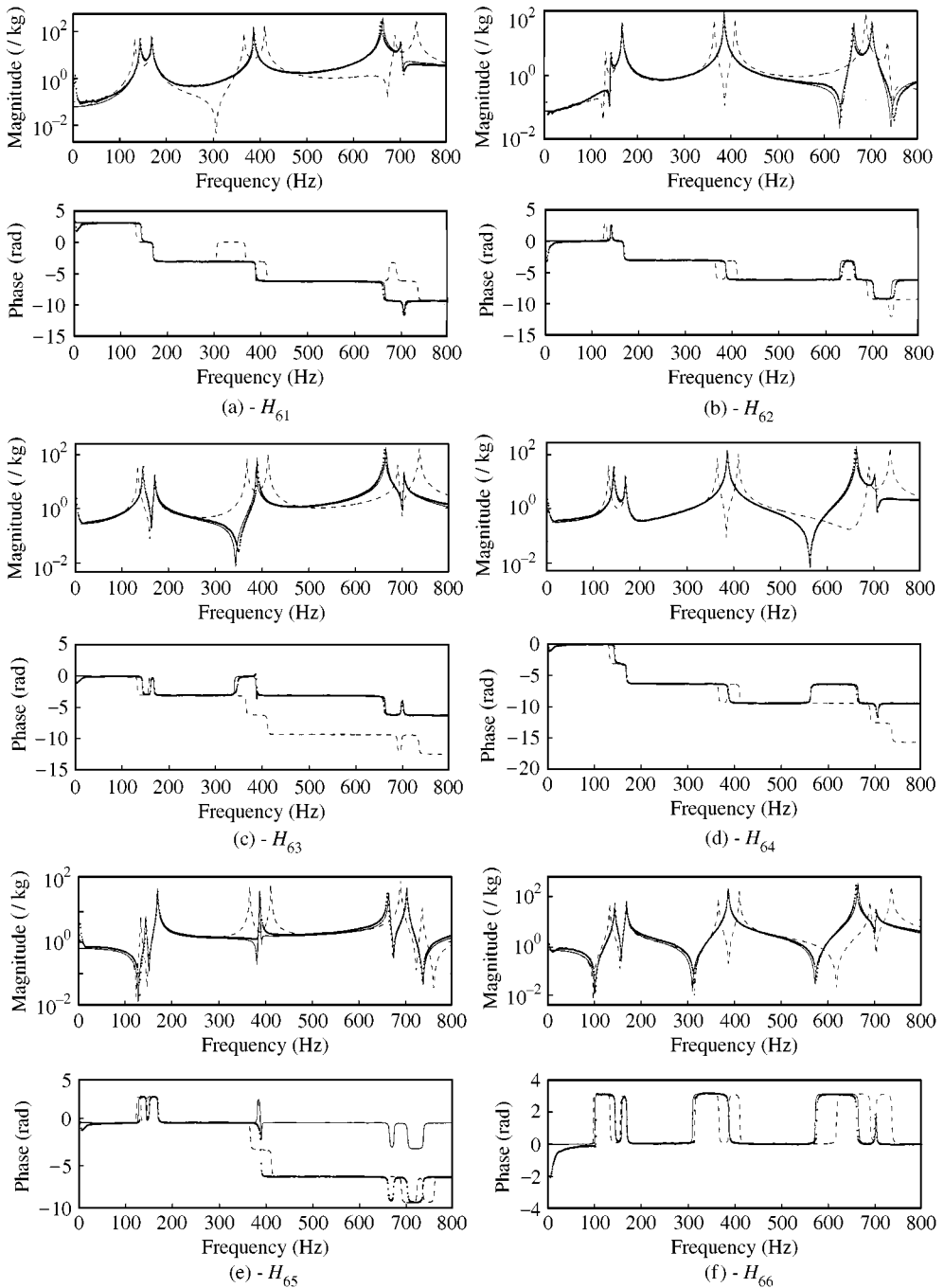


Figure 5. FRFs: original (— — —), test (· · · · ·) and updated (——). (a) H_{61} ; (b) H_{62} ; (c) H_{63} ; (d) H_{64} ; (e) H_{65} ; (f) H_{66} .

slightly decreased, even if some oscillation is noticed in the parameters updated using antiresonances (elements 13 and 16). Similarly, a slight stiffness decrease is shown by the slanted elements 7 and 11; for the last element, the decrease is larger when using the FRU-IT procedure, but this decrease is compensated by the increase of the adjacent element 10. For

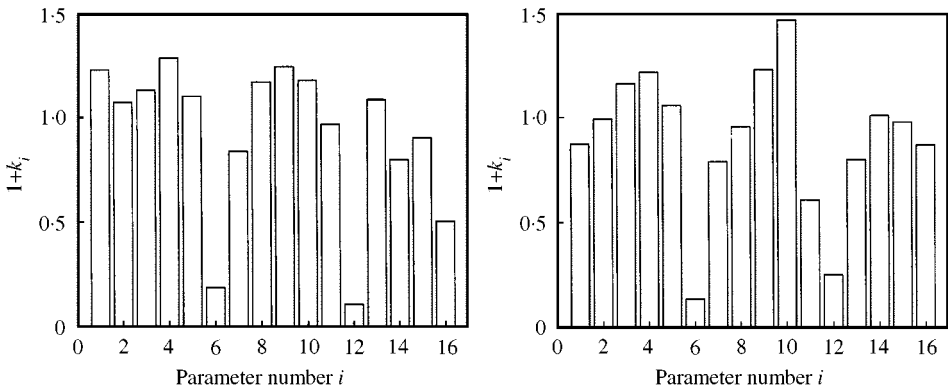


Figure 6. Stiffness correction factors: (left) updated using the present technique; (right) previously obtained using the FRU-IT technique and a different set of measurements.

the remaining elements, stiffness variations are of minor importance. Notwithstanding the similarities, the two sets of stiffness correction factors are different: the discussion about the uniqueness of the updated model could proceed indefinitely. However, it should be recalled that the compared results are obtained not only from different updating techniques, but also from different sets of measurements (point FRFs versus single reference modal testing, and impact excitation versus random excitation). It is enough to say that the identified natural frequencies are slightly different in the two cases!

3.3.2. Transfer FRFs

In this case the model is updated using antiresonances identified from the column of the FRF matrix corresponding to drive point 6. The number of identified antiresonances is 45 (12 of which are at 388 Hz) versus 72 when point FRFs were used. The overall number of data is $6 + 45 = 51$, giving rise to a maximum of 51 equations in 16 unknown parameters.

Obviously, the actual number of equations depends on the matching quality between analytical and experimental antiresonances. If some antiresonances remain unmatched after using FDAC, the number of usable data is lower.

In spite of using FDAC, convergence is not achieved unless the number of parameters to be updated is restricted through some parameters selection procedure, as in simulated tests. However, in this case the strategy of discarding the parameters that tend to diverge does not provide acceptable results. Better results are obtained by arbitrarily selecting the parameters on a presumed physical basis. Information from simulated tests is combined with that about uncertainties due to welded joints, leading to selection of the stiffness parameters of elements 2, 3, 4, 6, 8, 9, 10, 12.

The results are summarized in Figure 7 in terms of final errors on natural frequencies and antiresonances. Considering absolute values, the maximum error on natural frequencies is 1.83% and the average error is 0.49%, whilst for antiresonances the maximum error is about 4.51% and the average error is 0.85%. At the end of the process, all the 45 antiresonances are matched, whilst they were only 30 at the beginning.

If elements 7 and 11 are added to the previous set, convergence is achieved with more difficulty. The maximum error on natural frequencies is 1.74% and the average error is 0.48%, whilst for antiresonances the maximum error is about 4.39% and the average error is 0.96%. Apparently, results are better than in the previous case but now, at

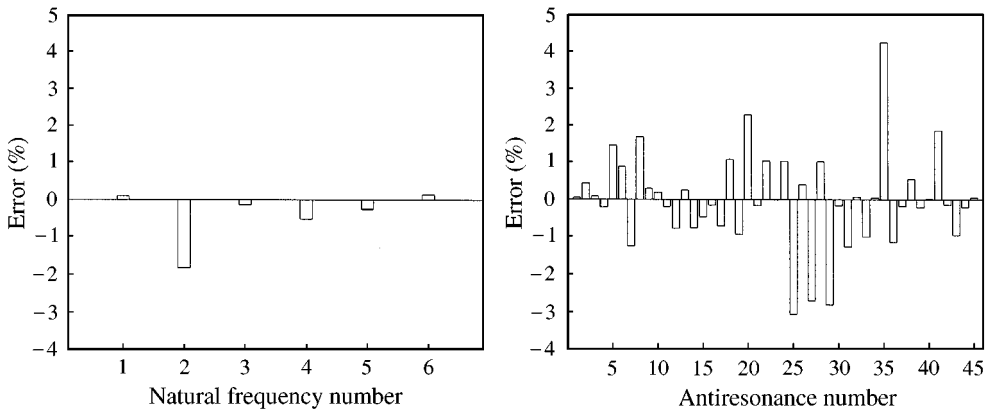


Figure 7. Final errors on natural frequencies (left) and antiresonances (right) using antiresonances identified from transfer FRFs.

the end of the process, only 39 antiresonances are matched. Therefore large invisible errors are present.

By considering the results of simulated and experimental tests for transfer FRFs, it is concluded that a general rule to perform parameter selection cannot be identified and this task must be developed on a case-by-case basis.

4. CONCLUSION

The use of antiresonances in the dynamic model updating of lightly damped structures seems to satisfy several demands. In fact, a good correlation between analytical and experimental antiresonances is of paramount importance in order to ensure the quality of dynamic models. On the other hand, the information provided by antiresonances is not independent of modal data, but antiresonances can be preferred to mode shapes because they are identified from experimental FRFs with much less error than the modes. Moreover, analytical antiresonances and their sensitivities are easily computed from the FE model.

However, the distribution of antiresonances in transfer FRFs can be significantly altered by small changes in the structural model. During the updating process, this makes it difficult to compute correctly the output residual because of possible mismatches between antiresonance pairs (test and analysis). One way to circumvent this problem is to restrict the experimental database to point FRFs. (In this case, transfer FRFs can eventually be used for the validation of the results.) Another approach consists of developing a procedure to deal with antiresonances identified from transfer FRFs. It attempts to match between test and analysis antiresonances at each iteration, by using the frequency domain assurance criterion to establish if their deformation shapes are well correlated or not.

The procedure using point FRFs is very robust and uses a complete set of information. Moreover, for a fixed number of FRFs, the number of involved antiresonances is maximum and it is maintained during the iteration process. However, point FRFs require experimental tests to be planned differently from the usual modal testing, with possible impact on the related costs.

The procedure using transfer FRFs is less robust than the one involving only point FRFs. Some antiresonances can be ignored due to lack of correlation and, moreover, the set of correlated antiresonances can be modified during the iteration process.

Results from both simulated and experimental data confirm what was previously stated.

With reference to simulated data, when point FRFs are used, errors on the updated parameters are of the same order as estimation errors on natural frequencies and antiresonances. Numerical stability is not affected by the initial value of the parameters and it is obtained without strictly limiting the step length at each iteration. On the contrary, using transfer FRFs, the FDAC is not sufficient to ensure convergence unless the initial estimate of the parameters is very close to their exact values, and in spite of strictly limiting the step length at each iteration. In this case, it is necessary to restrict the number of structural parameters to be updated.

Results obtained using antiresonances identified from measured point FRFs are highly satisfactory. The correlation between test and analysis FRFs is excellent both for point and transfer FRFs, where antiresonances are not explicitly considered by the updating procedure. The final values of the updated parameters can be interpreted as being due to welding faults and are not dissimilar to those previously obtained using a different technique and a different set of measurements. On the other hand, when using antiresonances identified from a measured column of the FRF matrix, it is again necessary to restrict the number of parameters to be updated, but the selection must be performed on a case-by-case, since no general rule can be identified for this task.

ACKNOWLEDGMENTS

This research is supported by MURST (Italian Ministry for University and Scientific Research) grants.

REFERENCES

1. W. D'AMBROGIO and A. FREGOLENT 1998 *Mechanical Systems and Signal Processing* **12**, 203–222. On the use of consistent and significant information to reduce ill-conditioning in dynamic model updating.
2. G. LALLEMENT and S. COGAN 1992 *10th IMAC, San Diego, U.S.A.*, 487–493. Reconciliation between measured and calculated dynamic behaviours: enlargement of the knowledge space.
3. J. E. MOTTERSHEAD 1998 *Mechanical Systems and Signal Processing* **12**, 591–597. On the zeros of structural frequency response functions and their sensitivities.
4. W. D'AMBROGIO and A. FREGOLENT 1999 *2nd International Conference on Identification in Engineering Systems, Swansea, U.K.*, 112–121. Promises and pitfalls of antiresonance based dynamic model updating.
5. D. J. NEFSKE and S. H. SUNG 1996 *Proceedings of the 14th International Modal Analysis Conference, Dearborne, U.S.A.*, 597–602. Correlation of coarse-mesh finite element model using structural system identification and a frequency response criterion.
6. R. PASCUAL, J. C. GOLINVAL and M. RAZETO 1997 *Proceedings of the 15th International Modal Analysis Conference, Orlando, U.S.A.*, 587–592. A frequency domain correlation technique for model correlation and updating.
7. Y. HALEVI and R. KENIGSBUCH 1999 *Proceedings of the 2nd International Conference on Identification in Engineering Systems, Swansea, U.K.*, 251–260. Model updating of the complex modeshapes and the damping matrix.
8. M. H. RICHARDSON and D. L. FORMENTI 1982 *Proceedings of the 1st International Modal Analysis Conference, Orlando, U.S.A.*, 167–186. Parameter estimation from frequency response measurements using rational fraction polynomial.
9. A. CARCATERRA and W. D'AMBROGIO 1992 *Proceedings of the 17th International Seminar on Modal Analysis, Leuven, Belgium*, 1115–1129. An iteration technique for the enhancement of the rational fraction polynomial modal identification procedure.
10. J. H. WILKINSON 1965 *The Algebraic Eigenvalue Problem*. Oxford, U.K.: Oxford University Press.

11. R. J. ALLEMANG and D. L. BROWN 1982 *Proceedings of the 1st International Modal Analysis Conference, Orlando, U.S.A.*, 110–116. A correlation coefficient for modal vector analysis.
12. D. J. EWINS 1997 *Proceedings of the 6th International Conference on Recent Advances in Structural Dynamics, Southampton, U.K.* Recent advances in modal testing.
13. A. FREGOLENT and W. D'AMBROGIO 1997 *Proceedings of the 16th Biennial ASME Conference on Mechanical Vibration and Noise, Sacramento, U.S.A., Paper No. DETC97-VIB4154*. Evaluation of different strategies in the parametric identification of dynamic models.
14. R. H. PLAUT and K. HUSEYIN 1973 *AIAA Journal* **11**, 250–251. Derivatives of eigenvalues and eigenvectors in non-self-adjoint systems.